THE UNIVERSITY *of* EDINBURGH

Edinburgh Research Explorer

On Evaluation of Power Electronic Devices' Efficiency for Nonsinusoidal Voltage Supply and Different Operating Powers

On Evaluation of Power Electronic Devices' Efficiency for Nonsinusoidal Voltage Supply and Different Operating Powers

Sasa Djokic, *Senior Member, IEEE*, Robert Langella, *Senior Member, IEEE*, Jan Meyer, *Senior Member, IEEE*, Robert Stiegler, Alfredo Testa, *Fellow, IEEE*, and Xiao Xu

Abstract—This paper analyses the impact of operating modes and nonideal power supply conditions on the efficiency of modern low-voltage power electronic devices. The sophisticated circuits and controls implemented in such devices are expected to result in increased efficiencies, higher operating power factors, and reduced harmonic emissions. However, the interactions of individual PE devices with the supplying network will impact exchanges of powers at fundamental system frequency and nonfundamental (i.e., harmonic) frequencies. This paper correlates the obtained results for harmonic performance and efficiencies over the entire range of operating powers of the considered PE devices using both standard definitions and some alternative interpretations.

Index Terms—Efficiency, harmonics, operating mode, power electronic (PE) devices, power-dependent characteristics.

NOMENCLATURE

PE	Power electronic (device).
LV	Low voltage.
PVI	Photovoltaic inverter.
SMPS	Switch-mode power supply.
WF1	Test voltage waveform 1 (sinusoidal).
WF2	Test voltage waveform 2 ("flattened top").
WF3	Test voltage waveform 3 ("pointed top").
PFC	Power factor correction/control.
MPPT	Maximum power point tracking.
THD_I	Total harmonic distortion of current.
P_{rated}	PE device rated power.
Z_s	Supply network impedance.
$P_{\text{PE,in/out}}$	PE device input–output power.
$P_{N,\text{in/out}}$	Input–output power through Z_s.
ΔP_N^1	Power dissipated on Z_s.
$P_{\text{PE,in/out}}^1$	PE device input–output fundamental active power.
$P_{\text{PE,in/out}}^h$	PE device input–output harmonic active power.
$\eta_{\text{PE,I/R}}$	Total efficiency of a PE device operated in inverter/rectifier mode.
$\eta'_{\text{PE,I/R}}$	Total fundamental efficiency of a PE device operated in inverter/rectifier mode.
$\eta_{N,I/R}$	Network efficiency for PE device operated in inverter/rectifier mode.
$\eta'_{N,I/R}$	Network fundamental efficiency for PE device operated in inverter/rectifier mode.
η_G	Global efficiency.
$P_{\text{AC,ref}}$	Reference ac active power.
$P_{\text{DC,ref}}$	Reference dc active power.
η_{ref}	Reference efficiency.
ΔP_{AC}	AC-power expanded uncertainty.
ΔP_{DC}	DC-power expanded uncertainty.
$\Delta \eta$	Efficiency expanded uncertainty.
η_{EU}	European Efficiency.
η_{CEC}	Californian Energy Commission Efficiency.

I. INTRODUCTION

An increasing number of modern low voltage (LV) power electronic (PE) devices utilizes sophisticated control circuits for improved performance and better regulation of grid-side ac currents. The implementation of these controls usually results in additional costs, which are generally justified by improved device efficiency and controllability, as well as by achieving reduced harmonic emissions during operation. Consequently, it is expected that both passive (i.e., power consuming) and active (i.e., power generating) modern PE devices will have low harmonic emissions and operate with high efficiencies [1], [2].

The test results from [3] and [4], however, demonstrated that some PE devices (e.g., photovoltaic inverters, PVIs) exhibit distinctive power-dependent changes of performance, typically manifested by the increased harmonic and interharmonic emissions in low-power operating modes (defined as 10%–30% of the rated power, P_{rated}), which might become particularly pronounced in very low-power modes (defined as <10% of P_{rated}). The actual grid supply conditions, i.e., the presence of voltage waveform distortions and unbalances, or variations in supply voltage magnitudes, had an additional impact on the characteristics of the tested PVIs.

The evaluation of efficiency of modern PE devices is an open metrological problem, which has wide practical implications for both standard equipment compliance laboratory testing and field verification of operational efficiency. The provision of accurate information on efficiency is particularly important in the context of the recent efforts aimed at impacting customers' choices in selecting electrical equipment offered on the market (and in that way, market sales), as reflected by, e.g., introduction of "Energy Label" in European Union (EU) [5], or "EnergyGuide" and "Energy Star" labels in U.S. [6]. Accordingly, a number of references analyzed various aspects of efficiency of PE devices ([7]–[27], see the following section) but, to the best knowledge of the authors, little attention has been devoted to the "fairness" of the metric to be adopted for the efficiency evaluation of commercial PE devices, as discussed in [7] and [8].

This paper builds on the initial results and analysis presented in [4], which are here significantly extended by providing: 1) a new section with a brief literature overview; 2) complete description of the applied measurement, instrumentation, data-processing procedures, and uncertainty analysis; 3) additional and more detailed results of measurements; and 4) further generalization of the concept of fundamental efficiency introduced in [9]. This is illustrated on several examples of commonly used active and passive PE devices (PVI and switch-mode power supply, SMPS), which are subjected to a comprehensive testing campaign, using test bed described in [3]. In all cases, an "ideally" sinusoidal waveform, WF1, was used as a reference, while the presence of realistic waveform distortions in ac supply voltage (so-called "background distortion") was emulated with two typically distorted voltage waveforms: WF2, with "flattened top," typical for LV networks supplying residential customers, and WF3, with "pointed top," typical for LV networks supplying industrial customers with a dominant share of line-commutating three-phase rectifiers. Two source impedance values are applied in tests: 1) minimum ($Z_{s1} \sim 0$) and 2) reference impedance Z_{s2} [28].

This paper is organized as follows. After a brief literature overview in Section III, Section IV presents the theoretical background for the evaluation of the efficiency under nonsinusoidal supply conditions and the analysis of measurement uncertainties on the efficiency evaluation. Section V reports the measurement results for the tested PE devices, while Section VI presents main conclusions.

II. BRIEF LITERATURE OVERVIEW

Efficiency of PVIs is discussed in terms of the actual static and dynamic dc-to-dc (i.e., maximum power point tracking, MPPT) and dc-to-ac conversion efficiencies, as well as their combination, i.e., the total PVI efficiency in [10]–[17]. Although a range of different factors was considered (e.g., input dc voltage, temperature, solar irradiance, partial shadowing, dust collection, differences from manufacturers' specification, and aging), reported PVI efficiency values (87%–99%) were given for operating powers greater than around 20%–50% of P_{rated}. Based on approaches from [18] and [19], known as European and Californian
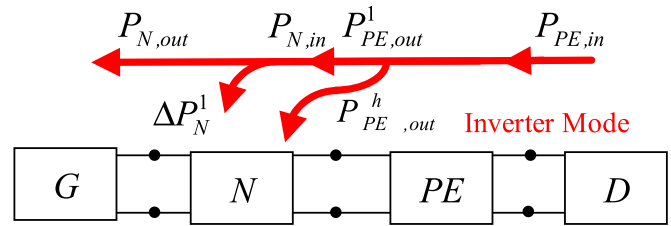

Fig. 1. Generalized power flows in the presence of PE interface operated in active/inverter mode assuming the absence of background distortion.

Efficiencies, in [20]–[23], PVIs' efficiencies are represented as averaged operating values for the assumed or calculated changes in annual distribution of input solar power, discussing their applicability for different geographic locations and climates. In case of SMPS, for which similar efficiency certification is given by, e.g., "80 Plus" labels [24], the evaluation of efficiencies is discussed in [25]–[27], again noticing that SMPS efficiency changes based on operating powers. It should be noted that the previous work assumed nominal voltage supply conditions (no or only very small background distortion and deviation from the nominal voltage) and did not analyze the impact of source impedance and different modes of operation due to applied SMPS controls.

Based on the initial results in [1]–[3], the efficiency of PVIs, SMPS, and electric vehicle battery chargers is in [4] evaluated in terms of the total harmonic distortion (THD_I) and source impedance values for different operating powers/modes, allowing to assess exchanges of powers at fundamental system frequency and nonfundamental (i.e., harmonic) frequencies. Reference [9] was made to the "total" device efficiency from the input to the output of the device, and to the "fundamental power" device efficiency. The same differentiation was made for supply network, introducing the total and fundamental power system efficiencies. Using the standard definitions and some alternative interpretations from [9], the harmonic performance and efficiencies of the considered PE devices are correlated in [4] and these initial results in this paper are discussed in more detail and illustrated with additional measurements.

III. EFFICIENCY EVALUATION FRAMEWORK

A. Theoretical Background

This section provides a generalization of the definitions from [9], applicable to any device (D), connected through a PE interface (PE), and a network impedance (N) to the grid supply (G) (Figs. 1 and 2).

Assuming the absence of background harmonic distortion, a PE device operated in active (i.e., inverter) mode (I), Fig. 1, will convert the input dc power $P_{\text{PE,in}}$ into the output ac power $P_{\text{PE,out}}$, which will be injected into the network at fundamental ($P_{\text{PE,out}}^1$) and all harmonic frequencies ($P_{P,\text{out}}^h$, the algebraic summation of all harmonic powers, with power directions positive in the direction of the fundamental power flow). Part of the fundamental power ΔP_N^1 and harmonic active power will be dissipated on the supply network impedance, with
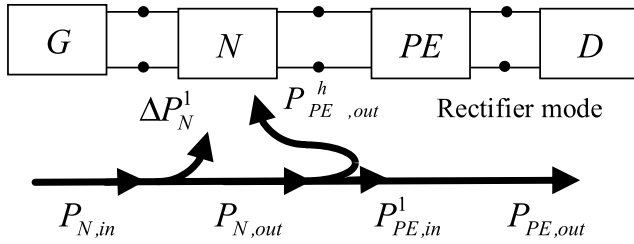
Fig. 2. Generalized power flows in the presence of PE interface operated in passive/rectifier mode assuming the absence of background distortion.

the remaining fundamental power $P_{N,\text{out}}$ flowing into the (sinusoidal) grid supply.

The total and the fundamental power efficiencies are

$$\eta_{\text{PE},I} = \frac{P_{\text{PE,out}}}{P_{\text{PE,in}}} = \frac{P_{\text{PE,out}}^1 + P_{\text{PE,out}}^h}{P_{\text{PE,in}}} \tag{1}$$

$$\eta'_{\text{PE},I} = \frac{P_{\text{PE,out}}^1}{P_{\text{PE,in}}^1} \tag{2}$$

where $\eta_{\text{PE},I}$—the total efficiency of a PE device operated in inverter mode, $P_{\text{PE,out}}$—the total output active power, $P_{\text{PE,in}}$—the total input active power, $P_{\text{PE,out}}^1$—the fundamental output active power, $P_{\text{PE,out}}^h$—the harmonic output active power, and $\eta'_{\text{PE},I}$—the fundamental power efficiency.

If the connected PE device is operated in passive (i.e., rectifier) mode (R), Fig. 2, input ac power is converted into dc and transferred to the supplied load/device (D), with harmonic power during the rectification stage taken from the supply grid and again dissipated on the supply network impedance N. The two efficiencies can be defined as

$$\eta_{\text{PE},R} = \frac{P_{\text{PE,out}}}{P_{\text{PE,in}}} = \frac{P_{\text{PE,out}}}{P_{\text{PE,in}}^1 + P_{\text{PE,out}}^h} \tag{3}$$

$$\eta'_{\text{PE},R} = \frac{P_{\text{PE,out}}}{P_{\text{PE,in}}^1}. \tag{4}$$

The corresponding network/system efficiencies are

$$\eta_{N,1} = \frac{P_{N,\text{out}}}{P_{N,\text{in}}}, \quad \eta'_{N,I} = \frac{P_{N,\text{out}}}{P_{N,\text{in}}^1} \tag{5,6}$$

$$\eta_{N,R} = \frac{P_{N,\text{out}}}{P_{N,\text{in}}}, \quad \eta'_{N,R} = \frac{P_{N,\text{out}}^1}{P_{N,\text{in}}}. \tag{7,8}$$

The symbols in (3) and (4) and (5)–(8) have the same meanings as in (1) and (2), but are written with corresponding subscripts for PE device operated in rectifier mode and for the network, respectively.

It is straightforward to demonstrate that the "global efficiency" is independent on the type of the device (active or passive)

$$\eta_G = \frac{P_{\text{out}}}{P_{\text{in}}} = \eta_N \cdot \eta_{\text{PE}} = \eta'_N \cdot \eta'_{\text{PE}}. \tag{9}$$

The question of selecting the most appropriate conversion efficiency for the analysis of PE devices (the one related to the total active power, or the one related to the fundamental active power) is important for a number of reasons, e.g., for

TABLE I
STANDARD UNCERTAINTIES BASED ON DATASHEET [30]–[33]

Current clamps	DC&AC	E_{reading} ± 1 % of reading,	E_{range} ± 2 mA
Signal conditioning current	DC	± 0.02 % of reading	± 0.05 % of range
	AC	± 0.05 % of reading	± 0.01 % of range
Signal conditioning voltage	DC	± 0.05 % of reading	± 0.05 % of range
	AC	± 0.05 % of reading	± 0.01 % of range
ADC	DC&AC	± 0.02 % of reading	± 0.013 % of range

evaluating general performance of PE device, for assessing "fairness" of electricity bills, and for estimating impact on the grid [7], [8].

Equations (1) and (3) are coherent with a calorimetric approach, indicating only the power losses within the PE device, while parts of the power dissipated in the supplying network are not apprehended. A more "fair" approach should refer to the definition of efficiency based on the fundamental power, i.e., (2) and (4), as it implicitly takes into account harmonic emissions and interactions between the grid and device (i.e., "polluting responsibilities").

For example, for a PE device operated in a rectifier mode under sinusoidal conditions of the grid supply and $Z_s \neq 0$, if P^h is negative (PE device is absorbing power at fundamental and injecting power at harmonic frequencies), $\eta'_{\text{PE}} < \eta_{\text{PE}}$, correctly "penalizing" the polluting device.

The situation is different when a background harmonic distortion is present. Assuming that the device has positive P^h (i.e., PE device is absorbing at both fundamental and harmonic frequencies due to the presence of supply network distortion), $\eta'_{\text{PE}} > \eta_{\text{PE}}$, correctly "rewarding" the device that is suffering from a polluting supply network. Obviously, it is well known that in real systems, the sign of the harmonic power can be positive or negative, depending on the interaction between the distorted supply network (in terms of both amplitudes and phase angles) and the PE device. Similar analysis applies for a PE device operated in active/inverter mode, with P_{PE}^h in the numerator in (1).

B. Evaluation of Measurement Accuracy and Uncertainties

The combined standard uncertainty of used measuring chain is determined by Monte Carlo (MC) simulations [29], starting from the standard uncertainties of: 1) current clamps; 2) signal conditioning modules; and 3) analog–digital conversion. MC simulations have been performed to determine how the uncertainties "propagate" to the calculation of ac and dc powers and to the calculation of the total and fundamental efficiencies. Since systematic errors have been compensated based on a detailed characterization of the measurement system, the datasheet uncertainties reported in Table I (E_{reading} and E_{range} are the standard uncertainties depending on reading and on range, respectively [30]–[33]) have been used to define—for the specific readings and ranges utilized—the distribution borders of the corresponding uniformly distributed random variables.

In order to obtain a representative set of results, in total 50 000 MC trials have been performed, including those with
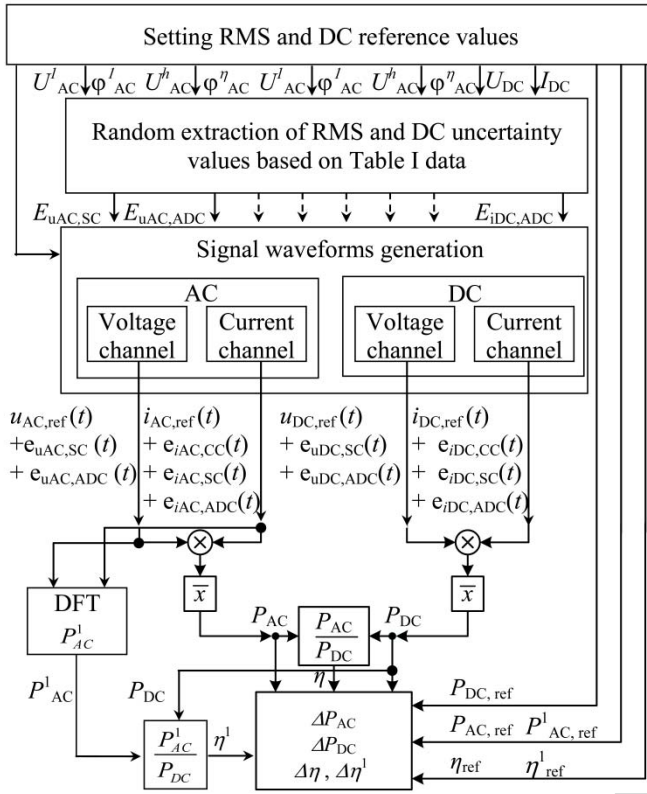
Fig. 3.   Algorithm implemented for each trial of the MC simulations.

Fig. 4.   Histogram and fit normal distribution of ac-power deviation, dc-power deviation, and efficiency deviation for an example of $P_{\mathrm{AC,ref}} = 460$ W, $P_{\mathrm{DC,ref}} = 474.22$ W, and $\eta_{\mathrm{ref}} = 0.97$ (see Fig. 3).

Fig. 5.   Expanded uncertainty (coverage probability of 95%) of simulated ac and dc powers for various power levels.

Fig. 6.   Expanded uncertainty (coverage probability of 95%) of simulated ac and dc powers and efficiency for an example of a fixed ac power of 690 W.

the presence of harmonics in voltages and currents (third and fifth harmonics, of amplitude 5% and 50% for voltage and current, respectively, with an angle between voltage and current harmonics of 0°, 90°, and 180°). The fundamental frequency has been considered exactly 50 Hz, since the experimental results reported in this paper refer to laboratory test conditions, in which the fundamental frequency is very accurately controlled by the power amplifier used (50 Hz $\pm$ 2 $\times$ 10^{-5} Hz).

Fig. 3 shows the implemented algorithm, which is used in each MC simulation trial. First, the input data of the reference signals are set in terms of rms values of the fundamental and harmonic components for ac signals and in terms of dc components for dc signals. Then, for each element of the measurement chain, random values of rms and dc uncertainty values are extracted in the interval $\pm[E_{\mathrm{reading}} + E_{\mathrm{range}}]$, based on the manufacturers' datasheet specifications (Table I) and on the reference rms or dc values. Afterward, ten cycles of the fundamental frequency time-domain signals are generated according to the sampling frequency chosen f_s both for the reference signals and for the corresponding uncertain signals. Finally, the deviations of the simulated values from the reference values are evaluated for all quantities of interest ΔP_{ac}, ΔP_{dc}, $\Delta \eta$, and $\Delta \eta^1$.

As an example, Fig. 4 shows the histograms of the ac and dc powers and efficiency deviations together with the fit normal distribution for a given set of reference signals and for a particularly critical working condition (low-power absorption). It is worth noting that the experimental distributions cannot be considered Gaussian, so reference is made to expanded
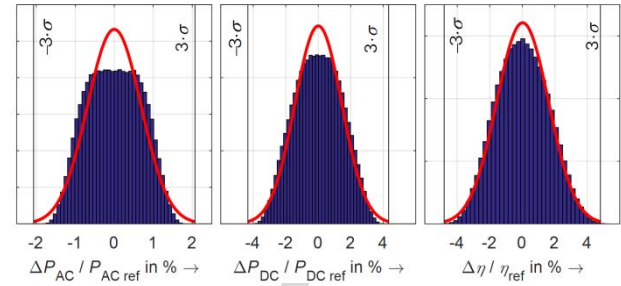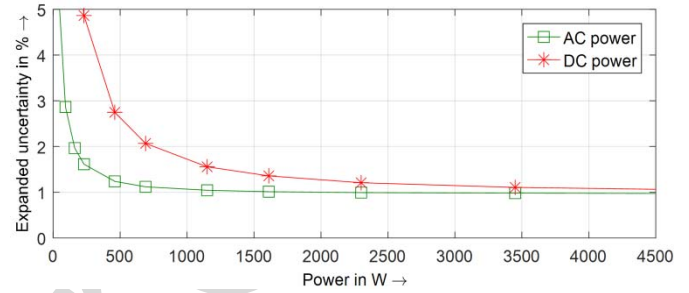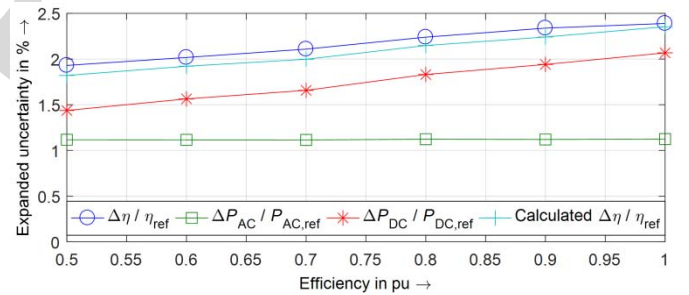
uncertainties calculated as the half of the coverage intervals corresponding to a coverage probability equal to 95%.

Fig. 5 shows the expanded uncertainty values for simulated ac and dc powers at different power levels. Obviously, the expanded uncertainty is decreasing with an increase of the power.

The following combined standard uncertainties could be derived from the previous analysis:

1) less than 0.9% for dc and 0.6% for ac powers for power values higher than 1 kW;
2) less than 2.5 % for dc and 0.9% for ac powers for power values between 250 W and 1 kW.

Fig. 6 shows the expanded uncertainty values for ac power, dc power, and efficiency η, respectively, as a function of efficiency for a fixed ac power of 690 W; the expanded uncertainty values of the efficiency are also calculated by the
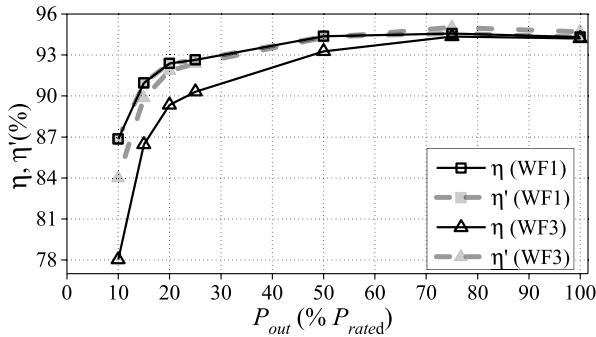
Fig. 7. Efficiencies of the tested PVI for WF1 and WF3 with Z_{s2}.

Fig. 8. THD$_I$ and P^h/P_{out} values of the tested PVI (WF1 and WF3 with Z_{s2}).

error summation law (10)

$$\frac{\Delta\eta}{\eta_{\text{ref}}} = \sqrt{\left(\frac{\Delta P_{\text{ac}}}{P_{\text{ac,ref}}}\right)^2 + \left(\frac{\Delta P_{\text{dc}}}{P_{\text{dc,ref}}}\right)^2}. \qquad (10)$$

It is worth noting that the results obtained for η with the MC simulations are close and conservative with respect to those obtained by (10).

Similar results have been obtained for fundamental ac power, dc power, and η^1; the fundamental efficiency values are also calculated by the summation low

$$\frac{\Delta\eta^1}{\eta_{\text{ref}}} = \sqrt{\left(\frac{\Delta P_{\text{ac}}^1}{P_{\text{ac,ref}}^1}\right)^2 + \left(\frac{\Delta P_{\text{dc}}}{P_{\text{dc,ref}}}\right)^2}. \qquad (11)$$

As the focus of this paper is the comparison between η and η^1, and considering that the dc power is affected by the greatest uncertainties, the uncertainty of the ratio between η and η^1, as a measure of the validity of the comparisons, is introduced

$$\frac{\Delta\left(\frac{\eta^1}{\eta}\right)}{\frac{\eta_{\text{ref}}^1}{\eta_{\text{ref}}}} = \sqrt{\left(\frac{\Delta P_{\text{ac}}^1}{P_{\text{ac,ref}}^1}\right)^2 + \left(\frac{\Delta P_{\text{ac}}^h}{P_{\text{ac,ref}}^h}\right)^2}. \qquad (12)$$

The combined standard uncertainty of the ratio in (12) is independent of dc power and has the following values:

1) less than 1% for ac powers higher than 1 kW;

2) less than 1.5% for ac powers between 250 W and 1 kW. These values do not affect significantly the validity of the comparisons between η and η^1 reported in the following text.

IV. EFFICIENCY MEASUREMENTS AND ANALYSIS

A. Photovoltaic Inverters

The first tested PE device is a three-phase PVI with rated power of 10 kW. Fig. 7 shows a comparison of its fundamental and total PE efficiencies at different operating powers, for sinusoidal supply (WF1) and "pointed-top" (WF3) background distortion and with Z_{s2}. (The results for "flattened-top" WF2 are not reported for the sake of clarity.) Shown values are the total efficiencies, from the input dc side of the PVI (where the PV emulator was connected) to the output ac side (including the MPPT efficiency).

It is possible to observe that the efficiencies η' and η are equal for sinusoidal supply voltage (WF1), while they
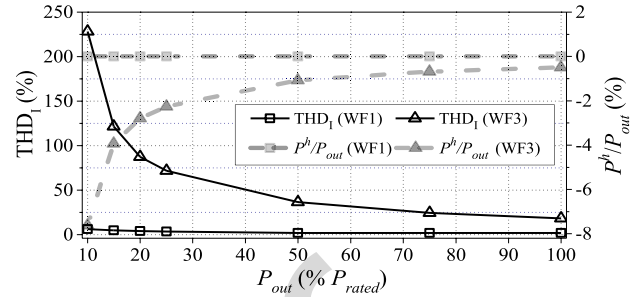
TABLE II
EU EFFICIENCY WEIGHTING FACTORS [18]

P/P$_{\text{rated}}$	5%	10%	20%	30%	50%	100%
Weight	0.03	0.06	0.13	0.10	0.48	0.20

show significant differences due to the presence of background voltage distortion (results for WF3). The main reason for the differences between η' and η for WF3 is related to the sign/flow of the harmonic power, which is negative for WF3, demonstrating that the inverter is behaving like a load (consuming harmonic powers from the grid). Value of η' for WF3 approaches η' for WF1, showing that the reduction of η for WF3 is a consequence of the background distortion. Moreover, for operating powers higher than 50%, the fundamental efficiency is almost constant and shows virtually no dependence on supply voltage distortion. Fig. 8 reports THD$_I$ and P^h/P values versus the output power of the tested PVI for sinusoidal supply conditions (WF1) and for distorted supply voltage condition (WF3).

Comparing results in Fig. 8, it is possible to observe the correlation among harmonic powers, THD$_I$ values and efficiencies. In particular, it can be clearly seen that PVI, as an example of "active" PE device with relatively high rated power, absorbs harmonic powers from the supply in the presence of supply voltage distortion (note negative sign of y-axis in Fig. 8), while injecting power at the fundamental frequency. In very low-power mode, sum of its harmonic powers amounts to around 10% of its total power.

Based on the previous considerations and on the well-known fact that the PVIs do not operate at their maximum/rated power, but change efficiency as a function of the operating power, the "European Efficiency—η_{EU}" and the "Californian Energy Commission Efficiency—η_{CEC}" have been introduced. They represent averaged operating efficiencies over a yearly power distribution corresponding to middle-Europe climate and Californian climate, respectively.

The EU efficiency was proposed by the Joint Research Center (JRC/Ispra), based on the Ispra climate model, and is now referenced on almost all inverter datasheets on the market. It combines the weighted inverter efficiency at six operating powers (Table II).

The CEC efficiency was proposed by the Californian Energy Commission and is based on the same approach

TABLE III
CEC Efficiency Weighting Factors [19]

P/P_{rated}	10%	20%	30%	50%	75%	100%
Weight	0.04	0.05	0.12	0.21	0.53	0.05

TABLE IV
Evaluation of Efficiencies

Grid supply	WF1		WF3	
Efficiency	η	η'	η	η'
Manufacturer (Rated), η_R	95.9	N/A	95.9	N/A
Manufacturer (Rated), $\eta_{R,EU}$	95.4	N/A	95.4	N/A
Max, η_{MAX}	94.6	94.6	94.4	95.0
EU, η_{EU}	92.1	92.1	89.0	90.4
CEC, η_{CEC}	93.9	93.9	92.8	94.0
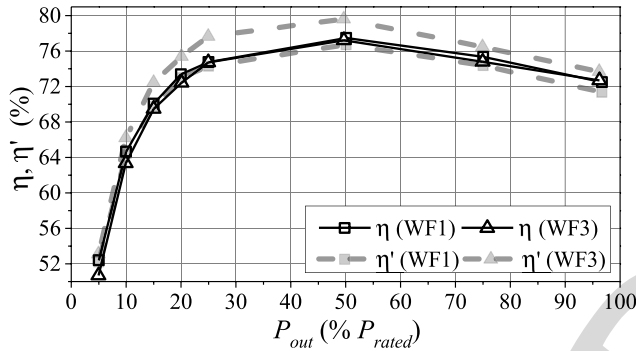
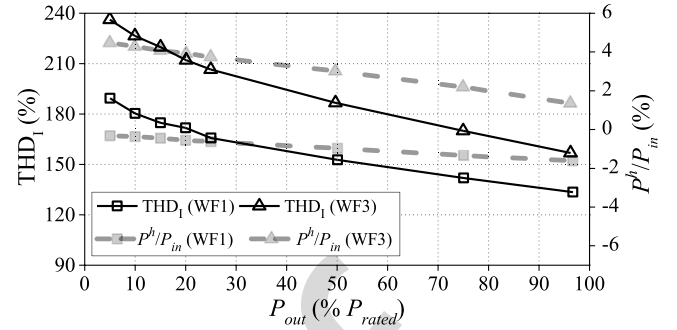Fig. 9.   Efficiencies of a 280-W SMPS with no-PFC (WF1 and WF3 with Z_{s2}).

Fig. 10. THD_I and P^h/P_{in} values of a 280-W SMPS with no-PFC (WF1 and WF3 with Z_{s2}).

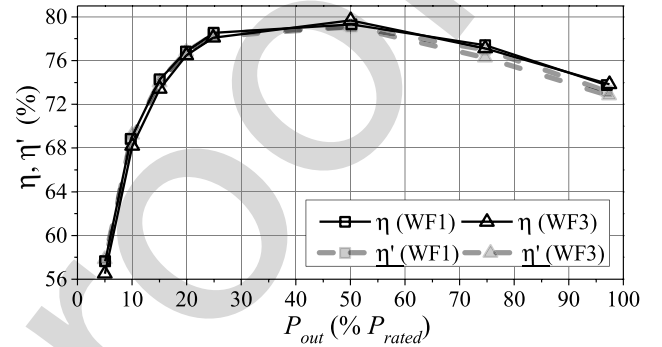Fig. 11.   Efficiencies of a 400-W SMPS with p-PFC (WF1 and WF3 with Z_{s2}).

as EU efficiency, but allocates higher weighting factors for $P/P_{\text{rated}} > 0.5$ pu. The total of six operating powers is considered, but 5% point is not considered, while a weighting factor at 75% is introduced (Table III).

Table IV compares the efficiency values reported by the manufacturer of the tested PVI and the measured maximum, and EU and CEC total and fundamental efficiencies, for WF1 and WF3 supply conditions, respectively.

From the results in Table V, it can be observed that all measured efficiencies (last three rows) are lower than the manufacturer-stated rated and EU efficiencies (third and fourth rows). As expected, under ideally sinusoidal supply conditions, there is no difference between the total and fundamental efficiencies. On the other hand, under distorted supply voltage conditions (i.e., for WF3), differences of about 0.6%, 1.4%, and 1.2% between the total and fundamental efficiencies are evaluated for η_{MAX}, η_{EU}, and η_{CEC}, respectively. Moreover, measured EU efficiency is up to 6.4% lower than the manufacturer's EU efficiency (89% versus 95.4%).

Finally, it is worth observing that even if these differences seem not too big, their economic implications (e.g., over one year of production or during the lifetime of installation) can be significant.

B. Switch-Mode Power Supplies

Figs. 9 and 10 are equivalent to Figs. 7 and 8 for a 280-W SMPS without power factor correction/control (PFC) circuit, as found before the introduction of the IEC Standard 61000-3-2 ([34]) in the EU, which sets limits for current harmonics emission (up to the 40th harmonic), with "Class D" applying to SMPS found in desktop PCs. As in the case of PVI, illustrated values are total efficiencies, measured from the input ac side to the output dc side of the tested SMPS.

It is possible to observe, as in the case of the PVI, that there are no significant differences between η and η' under sinusoidal supply conditions (WF1), as well as for η under distorted conditions (WF3). However, in this case, the fundamental efficiency η' under distorted conditions (WF3) is higher. This can be explained by results in Fig. 10, where it is possible to observe that the SMPS absorbs harmonic powers from the supply in the presence of supply voltage distortion (note positive sign of right y-axis for WF3). On the other hand, the SMPS injects harmonic power under sinusoidal supply conditions (negative sign), as the most of the "passive" PE devices. These results confirm that (4) is again more "fair" than (3), as the SMPS is "victim" of the background distortion.

Figs. 11 and 12 show the similar results for a 400-W SMPS with passive PFC (p-PFC) circuit. In this case, all of the calculated efficiencies almost coincide, but Fig. 12 clarifies that under sinusoidal supply conditions (WF1), the harmonic power is almost zero, while under distorted conditions (WF3), the harmonic power is lower than for the SMPS without PFC and changes the sign from negative to positive during the transfer from the lower to the higher operating powers.

Figs. 13 and 14 report the results for a modern SPMS with active PFC (a-PFC) circuit. Both fundamental efficiency η'
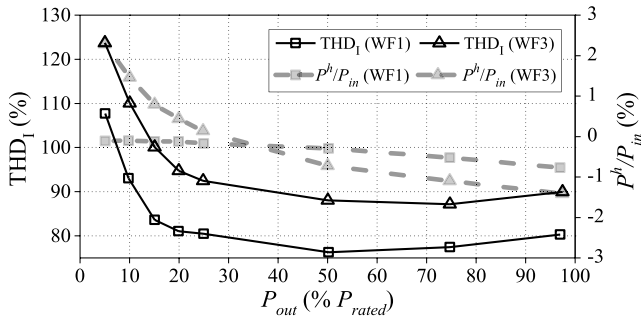
Fig. 12. THD_I and P^h/P_{in} values of a 400-W SMPS with p-PFC for WF1 and WF3 with Z_{s2}.
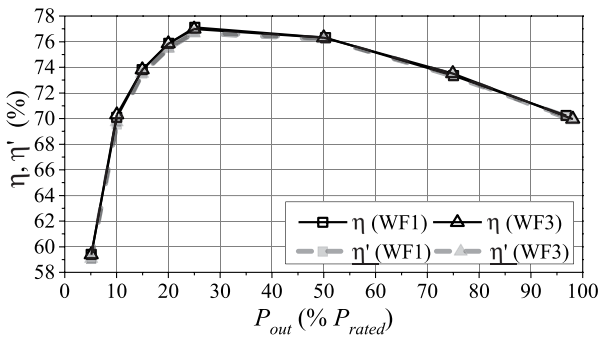

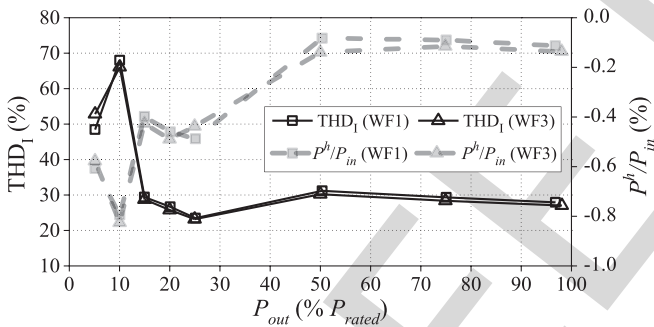Fig. 13. Efficiencies of a 400-W SMPS with a-PFC (WF1 and WF3 with Z_{s2}).

Fig. 14. THD_I and P^h/P_{in} values of a 400-W SMPS with a-PFC (WF1 and WF3 with Z_{s2}).

and total efficiency η do not show any significant difference among each other, with no evident dependence on the presence/absence of supply voltage distortion, confirming that active PFC technology reduces both the THD_I and the flow of harmonic power.

V. Conclusion

This paper presents an experimental evaluation and subsequent analysis of obtained test results aimed at assessing the impact of operating modes and nonsinusoidal voltage supply conditions on the efficiency of modern LV PE devices. Two commonly found types of modern PE devices are tested and analyzed, representing both passive, i.e., power-consuming equipment (SMPS rectifiers) and active, i.e., power-generating equipment (PV inverters).

The sophisticated electronic circuits and versatile controls implemented in these modern PE devices are expected to result in increased efficiency, higher operating power factors, and reduced harmonic emissions. However, the presented analysis shows that the interactions of individual PE devices with the supplying network result in power-dependent change in performance, manifested through the exchanges of powers at both fundamental system frequency and nonfundamental (i.e., harmonic) frequencies. Based on this analysis, this paper correlates the obtained results for harmonic performance and efficiencies over the entire range of operating powers of the considered PE devices, using both standard definition of efficiency and a generalized alternative interpretation.

This paper provides detailed description of the test conditions, with particular attention to the analysis and evaluation of uncertainties of the experimental setup. Although one of the main motivations of this paper was to reproduce realistic supply conditions (e.g., the presence of source impedance and background distortion), not all of the impact parameters present in the field are considered in the laboratory. These include: nonsteady-state operating points of PE devices, temporal variations in the background distortion, and fundamental frequency variations, which would require further analysis in terms of its influence on the measurement results.

From the metrological point of view, the problem of selecting the most appropriate metric for evaluating (conversion) efficiency of PE devices is discussed based on the use of "standard" total power/device efficiency (η) and generalized concept of fundamental power efficiency (η'). The presented results demonstrate that both in the cases of PVI and SMPS, a "fairer" approach would be to use definition of efficiency based on the exchanges of fundamental power. Accordingly, this definition is recommended in this paper, as it takes into account in a more appropriate way harmonic emissions and interactions between the grid and the device (i.e., harmonic "pollution responsibilities").

From the point of view of related standards requirements and procedures, the presented results and analysis also raise an important question about the adequacy of current recommendations and procedures for the assessment of harmonic emission limits and electromagnetic compatibility (see [34]). Modern PE devices implement sophisticated controls, marking significant difference from the period as recent as one decade ago, when most PE equipment had only simple circuit topologies, without any PFC or with only passive PFC circuit implemented in equipment design. However, most of the related standards were developed several decades ago, which require only tests with ideally sinusoidal voltages and without source impedance, as these typically represented the conditions under which previous PE devices exhibited maximum harmonic emission levels.

If similar conditions are used for efficiency assessment of modern PE devices, the results can differ from the realistic (fundamental) efficiency that can be achieved during the field operation. Consequently, test conditions for efficiency assessment should also include typical supply voltage distortion, as found in the actual networks. A starting point for a suitable updating of testing conditions specified in standards could

be the definition of a flat-top waveform, as provided in the standard IEC 61000-4-13.

ACKNOWLEDGMENT

REFERENCES

[1] X. Xu *et al.*, "Analysis and modelling of power-dependent harmonic characteristics of modern PE devices in LV networks," *IEEE Trans. Power Del.*, vol. 32, no. 2, pp. 1014–1023, Apr. 2017.

[2] S. Yanchenko and J. Meyer, "Harmonic emission of household devices in presence of typical voltage distortions," in *Proc. IEEE PowerTech Conf.*, Eindhoven, The Netherland, Jun./Jul. 2015, pp. 1–6.

[3] R. Langella, A. Testa, J. Meyer, F. Möller, R. Stiegler, and S. Z. Djokic, "Experimental-based evaluation of PV inverter harmonic and interharmonic distortion due to different operating conditions," *IEEE Trans. Instrum. Meas.*, vol. 65, no. 10, pp. 2221–2233, Oct. 2016.

[4] X. Xu *et al.*, "On the impact of operating modes and power supply conditions on the efficiency of power electronic devices," in *Proc. Int. Workshop Appl. Meas. Power Syst. (AMPS)*, Aachen, Germany, Sep. 2016, pp. 23–25.

[5] Directive 2010/30/EU of the European Parliament and of the Council, "The indication by labelling and standard product information of the consumption of energy and other resources by energy-related products," *Off. J. Eur. Union*, May 2010.

[6] S. Vaidyanathan *et al.*, "Overcoming market barriers and using market forces to advance energy efficiency," Amer. Council Energy-Efficient Econ., Tech. Rep. E136, 2013.

[7] L. S. Czarnecki, "Comments on active power flow and energy accounts in electrical systems with nonsinusoidal waveforms and asymmetry," *IEEE Trans. Power Del.*, vol. 11, no. 3, pp. 1244–1250, Jul. 1996.

[8] R. Carbone, R. Langella, and A. Testa, "On the billing of electrical energy flows at prosumers' busbar," in *Proc. 14th Int. Conf. Harmon. Quality Power (ICHQP)*, Bergamo, Italy, Sep. 2010, pp. 1–7.

[9] R. Langella and A. Testa, "Switching power supplies: Analysis of waveform distortion and absorbed powers," in *Proc. 9th Int. Conf. Electr. Power Quality Utilization*, Barcelona, Spain, Oct. 2007, pp. 1–6.

[10] W. Mara?da and M. Piotrowicz, "Calculation of dynamic MPP-tracking efficiency of PV-inverter using recorded irradiance," in *Proc. 20th Int. Conf. Mixed Design Integr. Circuits Syst. (MIXDES)*, Gdynia, Poland, Apr. 2013, pp. 431–434.

[11] M. Valentini, A. Raducu, D. Sera, and R. Teodorescu, "PV inverter test setup for European efficiency, static and dynamic MPPT efficiency evaluation," in *Proc. 11th Int. Conf. Optim. Electr. Electron. Equip.*, Brasov, Romania, Sep. 2008, pp. 433–438.

[12] J. Muñoz, F. Martínez-Moreno, and E. Lorenzo, "On-site characterisation and energy efficiency of grid-connected PV inverters," *Progr. Photovol. Res. Appl.*, vol. 19, no. 2, pp. 192–201, 2011.

[13] Y. Dong, J. Huang, J. Ding, H. Li, and S. Zhang, "Performance test and evaluation of photovoltaic system," in *Proc. Int. Conf. Renew. Power Generat. (RPG)*, Beijing, China, 2015, pp. 1–4.

[14] A. E. Brooks *et al.*, "Conversion efficiencies of six grid-tied inverters at the Tucson electric power solar test yard," in *Proc. IEEE 39th Photovol. Specialists Conf. (PVSC)*, Tampa, FL, USA, Sep. 2013, pp. 2853–2856.

[15] B. Andò, S. Baglio, A. Pistorio, G. M. Tina, and C. Ventura, "Sentinella: Smart monitoring of photovoltaic systems at panel level," *IEEE Trans. Instrum. Meas.*, vol. 64, no. 8, pp. 2188–2199, Aug. 2015.

[16] L. Cristaldi, M. Faifer, M. Rossi, L. Ciani, M. Lazzaroni, and S. Toscani, "Photovoltaic plant efficiency evaluation: A proposal," in *Proc. 12th IMEKO TC10 New Perspect. Meas. Tools Techn. Ind. Appl.*, Florence, Italy, Jun. 2013, pp. 1–6.

[17] L. Cristaldi, M. Faifer, M. Rossi, and S. Toscani, "An improved model-based maximum power point tracker for photovoltaic panels," *IEEE Trans. Instrum. Meas.*, vol. 63, no. 1, pp. 63–71, Jan. 2014.

[18] R. Hotopp, *Private Photovoltaik-Stromerzeugungsanlagen im Netzparallelbetrieb: Planung, Errichtung, Betrieb, Wirtschaftlichkeit*, Essen, Germany: RWE, 1991.

[19] W. Bower, C. Whitaker, W. Erdman, M. Behnke, and M. Fitzgerald, "Performance test protocol for evaluating inverters used in grid-connected photovoltaic systems," Tech. Rep. REN-1038, Oct. 2004.

[20] I. Ongun, E. Özdemir, "Weighted efficiency measurement of PV inverters: Introducing ηIZMIR," *J. Optoelectron. Adv. Mater.*, vol. 15, nos. 5–6, pp. 550–554, May/Jun. 2013.

[21] L. Aarniovuori, A. Kosonen, P. Sillanpää, and M. Niemelä, "High-power solar inverter efficiency measurements by calorimetric and electric methods," *IEEE Trans. Power Electron.*, vol. 28, no. 6, pp. 2798–2805, Jun. 2013.

[22] B. Bletterie *et al.*, "Redefinition of the European efficiency—Finding the compromise between simplicity and accuracy," in *Proc. 23rd Eur. Photovolt. Solar Energy Conf. Exp. (PVSEC)*, Valencia, Spain, Sep. 2008, pp. 1–5.

[23] Z. Salam and A. Rahman, "Efficiency for photovoltaic inverter: A technological review," in *Proc. IEEE Conf. Energy Convers. (CENCON)*, Johor Bahru, Malaysia, Sep. 2014, pp. 175–180.

[24] A. Mansoor *et al.*, "Generalized test protocol for calculating the energy efficiency of internal Ac-Dc and Dc-Dc power supplies," EPRI/Ecova, Palo Alto, CA, USA, Tech. Rep., 2014.

[25] F. Khan, T. D. Geist, B. Vairamohan, B. D. Fortenbery, and E. Hubbard, "Challenges and solutions in measuring computer power supply efficiency for 80 PLUS certification," in *Proc. 24th. IEEE Conf. Expo. Appl. Power Electron.*, Washington, DC, USA, Sep. 2009, pp. 2079–2085.

[26] W. Konrad, G. Deboy, and A. Muetze, "A power supply achieving titanium level efficiency for a wide range of input voltages," *IEEE Trans. Power Electron.*, vol. 32, no. 1, pp. 117–127, Jan. 2017.

[27] S. Kawaguchi and T. Yachi, "Adaptive power efficiency control by computer power consumption prediction using performance counters," *IEEE Trans. Ind. Appl.*, vol. 52, no. 1, pp. 407–413, Jan./Feb. 2016.

[28] *Consideration of Reference Impedances and Public Supply of Network Impedance for Use in Determining Disturbance Characteristics of Electrical Equipment Having a Rated Current Less Than 75A Per Phase*, Standard IEC 60725, 2005.

[29] *JCGM 101:2008: Evaluation of Measurement Data—Supplement 1 to the Guide to the Expression of Uncertainty in Measurement—Propagation of Distributions Using a Monte Carlo Method*, 2008.

[30] *Voltage Modules (HSI-HV)*. [Online]. Available: https://ccc.dewetron.com/dl/53970d9a-fc10-44f0-a97f-0709d9c49861

[31] *Current modules (HSI-LV)*. [Online]. Available: https://ccc.dewetron.com/dl/53970d9a-05e0-44f1-b968-0709d9c49861

[32] *Current Transducers (PNA-Clamp-150-DC)*. [Online]. Available: http://www.dewesolutions.sg/uploads/7/7/1/6/7716986/dewetron-apps_power_pm_de_b090315e.pdf

[33] *DAQ board (DEWE-ORION-0816-100X)*. [Online]. Available: http://www.systemtech.se/fileadmin/resources/datasheets/dewetron/2011/dewetron_dewe-orion_e.pdf

[34] *Electromagnetic Compatibility (EMC), Part 3-2: Limits for Harmonic Current Emissions (Equipment Input Current Less Than or Equal to 16 A per Phase)*, document IEC 61000-3-2, 2009.

Sasa Djokic (M'05–SM'11) was born in Kosovska Kamenica, Serbia, in 1967. He received the Dipl.-Ing. and M.Sc. degrees in electrical engineering from the University of Nis, Nis, Serbia, in 1992 and 2001, respectively, and the Ph. D. degree electrical engineering from the University of Manchester Institute of Science and Technology, Manchester, U.K., in 2004.

He is currently a Reader of Electrical Power Systems with the University of Edinburgh, Edinburgh, U.K.

Dr. Djokic is a Senior Member of the IEEE Power Engineering Society.

Robert Langella (S'00–M'01–SM'10) was born in Naples, Italy, in 1972. He received the electrical engineering degree from the University of Naples, Naples, in 1996, and the Ph.D. degree in electrical energy conversion from the Second University of Naples, Aversa, Italy, in 2000.

He is currently an Associate Professor of Electrical Power Systems with the Second University of Naples.

Dr. Langella is a Senior Member of the IEEE Power Engineering Society.

Jan Meyer (M'11–SM'17) was born in Dresden, Germany, in 1969. He received the Dipl.-Ing. and Ph.D. degrees in electrical power engineering from the Technische Universitaet Dresden, Dresden, Germany, in 1994 and 2004, respectively.

He is currently a Senior Academic Assistant and a Team leader of Power Quality Research Group with the Technische Unversitaet Dresden.

He is a member of the IEEE Power Engineering Society.

Robert Stiegler was born in Wolmirstedt, Germany, in 1983. He received the Dipl.-Ing. degree from the Technische Universität Dresden, Dresden, Germany, in 2010, with a thesis on the development of a test system for accuracy verification of power quality instruments.

He is currently with the Institute of Electrical Power Systems, Technische Universität Dresden.

Alfredo Testa (M'83–SM'03–F'08) was born in Naples, Italy, in 1950. He received the degree in electrical engineering from the University of Naples, Naples, in 1975.

He is currently a Professor of Electrical Power Systems with the Second University of Naples, Aversa, Italy. He is involved in the research on electrical power systems reliability and harmonic analysis.

Dr. Testa is a fellow of the IEEE Power Engineering Society and the Italian Institute of Electrical Engineers (AEI).

Xiao Xu was born in China, in 1990. He received the B.Eng. degree in civil engineering from Nanjing Tech University, Nanjing, China, and the M.Sc. degree in sustainable energy systems from the University of Edinburgh, Edinburgh, U.K., where he is currently pursuing the Ph.D. degree.